Experimental and Computed Results Concerning the Diagnosis of Broken Rotor Bars of the Induction Motors.

*A. Ghoggal, **S. E. Zouzou, *M. Sahraoui,**A. Aboubou.
* Département d'Electrotechnique
Université Mentouri - Constantine
** Département d'Electrotechnique
Université Mohamed khider-Biskra
*E-mail: ghoetudes@yahooo.fr

H. Razik.
Groupe de Recherches en Electrotechnique
et Electronique de Nancy GREEN - UHP - UMR - 7037
Université Henri Poincaré - Nancy 1 - BP 239
F - 54506 Vandoeuvre-les-Nancy, Cedex, France
E-mail: Hubert.Razik@ieee.org

Abstract *- A model permitting the simulation of induction machine with skewed rotor slot is presented. The model is based on the Extension of the Modified Winding Function Approach, which allows for all harmonics of MMF to be taken into account. The effects of rotor skew which have not been able to be analyzed accurately by 2-D finite element technique were investigated. The model is used to predict the characteristics frequency components which are indicative of rotor bar faults. The experimental results obtained showed the importance of the method for the analysis of the induction motors.*

I. INTRODUCTION

The induction motor is a key component of the majority of the industrial plants, because of its great robustness and its low cost. It is indeed, omnipresent in the industrial sectors like aeronautics, the nuclear power, chemistry. In spite of these qualities, stresses of various natures (thermal, electrical, mechanical or environment) can affect the life span of this one by involving the occurrence of stator and/or rotor faults [1]. These faults cause considerable economic losses. Thus, it is imperative to implement monitoring systems in order to avoid the unforeseen stops. The usual method for stator and rotor faults detection is based on the motor current signature analysis (MCSA) [2]. For that, a model closer to reality must be established. Several studies was published in this axis, and made possible the detection of the various defects, while analyzing the frequencies higher or lower than the fundamental stator frequency. A model taking into account the real distribution of FMM is presented, it is based on an extension in 2D of the modified winding function approach, with the effects of the rotor skew and the eccentricity [3], [4], [5].

The expressions of the magnetizing inductances and mutual inductances are derived from an extension of the modified winding function approach. In the case of multiple coupled circuit model, an accurate calculation of the electromagnetic torque depends on the accuracy of inductances derivatives. The inductances matrixes as well as its derivative must be calculated at each integration step, it well known that the other method consume a high time, the proposed method is based in a simple and clever analytical calculation of a double integration witch will be the base of inductances calculation. This method can reduce the simulation time. The simulation tools are implemented using MATLAB language. Simulation and experimental results confirm the validity of this model.

II. INDUCTION MACHINE MODEL

Knowing that the cage can be viewed as identical and equally spaced rotor loops, it is possible to establish voltage equations of stator and rotor loops as [7]:

$$[U_s] = [R_s][I_s] + \frac{d[\psi_s]}{dt}, \quad (1)$$

$$[\mathbf{0}] = [R_r][I_r] + \frac{d[\psi_r]}{dt}, \quad (2)$$

$$[\psi_s] = [L_{ss}][I_s] + [L_{sr}][I_r], \quad (3)$$

$$[\psi_r] = [L_{rs}][I_s] + [L_{rr}][I_r]. \quad (4)$$

The vector $[U_s]$ corresponds to the stator voltages, $[I_s]$ and $[I_r]$ to the stator and rotor currents. m is the number of stator phases and N_b the number of rotor bars. $[R_s]$ is an m dimensional diagonal matrix, $[L_{ss}]$ is an $m \times m$ symmetric matrix, $[L_{sr}]$ is an $m \times (N_b + 1)$ matrix, and $[R_r]$ and $[L_{rr}]$ are $(N_b + 1) \times (N_b + 1)$ matrix. Adding to these equations the mechanical expression and the equations electromagnetic torque yields to:

$$C_e - C_r = J_r \frac{d\omega_r}{dt} \quad , \quad C_e = \left(\frac{dW_{co}}{d\theta_r} \right) \Bigg|_{(I_s, I_r = \text{constant})} \quad , \quad (5)$$

$$W_{co} = \frac{1}{2}([I_s]^T[L_{ss}][I_s] + [I_s]^T[L_{sr}][I_r] + [I_r]^T[L_{rr}][I_r] + [I_r]^T[L_{rs}][I_s]), \quad (6)$$

where W_{co} is the coenergy, C_e the electromagnetic torque, C_r the load torque, J_r the rotor load inertia, and ω_r the mechanical speed of the rotor.

III. MODELING OF INDUCTION MOTOR WITH SKEWED ROTOR SLOTS USING AN EXTENSION OF MODIFIED WINDING FUNCTION APPROACH (MWFA)

According [3],[14] and [15] it will be possible to lead to the expression of winding function:

$$N(\varphi, z, \theta_r) = n(\varphi, z, \theta_r) - \frac{1}{2\pi\ l\langle g^{-1}(\varphi, z, \theta_r)\rangle} \int_0^{2\pi} \int_0^{l} n(\varphi, z, \theta_r) g^{-1}(\varphi, z, \theta_r) dz d\varphi. \quad (7)$$

where, g is the air gap and l is the effective length. It is to be noticed that this new expression does not hold any restriction as for the axial uniformity, in particular in term of skewing slots and axial air-gap non uniformity. In this study, we take into account only the rotor skew and the opening of the slots, in the case of a constant air-gap.

By supposing that the machine is symmetrical, the air-gap length g is reduced to g_0 which is the radial air-gap length in the case of no eccentricity. If *F* is the MMF distribution in the air-gap due to the current i_{A_i} flowing in an arbitrary coil A_i, and knowing that the elementary flux corresponding in the air-gap is measured in comparison to an elementary volume of section *ds* and length g_0 such as

$$d\phi = \mu_0 F g_0^{-1} ds, \quad (8)$$

The calculation of total flux is made through a calculation of a double integral. By carrying out the change of variable $x = r\varphi$ and $x_r = r\theta_r$ the study is transformed to a reference with axes X and Z where we can imagine a plane representation of the machine. It is clear that, in this case, *x* translate correctly the linear displacement along the arc corresponding to the angular opening φ. It is the same thing concerning x_r and θ_r.

Knowing that N is the MMF per unit of current, the expression giving the flux seen by all the turns of coil B_j of winding *B* due to i_{Ai} flowing in coil A_i will be reduced as

$$\phi_{BjAi} = \frac{\mu_0}{g_0} \int_{x_{1j}}^{x_{2j}} \int_{z_{1j}(x)}^{z_{2j}(x)} N_{Ai}(x, z, x_r) n_{Bj}(x, z, x_r) i_{Ai} dz dx. \quad (9)$$

This is due to the fact that by taking into account the axial asymmetry $n_{Bj}(x, z, x_r)$ will be defined so as to be able to translate the skew of the slots. In 2-D, it will be written in the following way:

$$n_{Bj}(x, z, x_r) = \begin{cases} w_{Bj} & x_{1j} \langle x \langle x_{2j}\ ,\ z_{1j}(x) \langle z(x) \langle z_{2j}(x), \\ 0 & \text{in the remaining interval} \end{cases} \quad (10)$$

where w_{Bj} is the number of turns of coil B_j. It is equal to 1 in the case of a rotor loop. Generally, the total flux ψ_{BA} related to all coils composing winding A and *B*, holds its general expression by integrating over the whole surface. Then knowing that the mutual inductance L_{BA} is the flux ψ_{BA} per unit of current, yields

$$L_{BA}(x_r) = \frac{\mu_0}{g_0} \int_0^{2\pi r} \int_0^{l} N_A(x, z, x_r) n_B(x, z, x_r) dz dx. \quad (11)$$

Note that a rearrangement of (11) makes possible to define an inductance per unit of length as described in [4]:

$$L_{BA}(x_r) = \int_0^{l} L'_{BA}(z, x_r) dz. \quad (12)$$

According to the manner of connecting the coils translated by the sign in (13), this inductance can be obtained by summing all mutual inductances between the q and p coils of windings *A* and *B* respectively, such as:

$$L_{BA}(x_r) = \sum_{i=1}^{q} \sum_{j=1}^{p} \pm L_{B_j A_i}(x_r) \quad (13)$$

IV. SIMULATION RESULTS

The described method was applied to a three phases induction machine 3 kW, tow poles, 230/400v, 2800tr/mn, 50Hz, Nb=28, skewed rotor. Machines parameters are given in the Appendix. Fig. 1 illustrates the functions which describe the mutual inductances L_{r1A} between the first stator phase A, and the first rotor loop, in the four cases considered, without and with taking into account the slots opening and the skewing of rotor bares. A rotor loop is regarded as being a coil with one turn. Note that the mutual inductance between phase and the second rotor loop is the same as it was given in Fig. 1, but shifted to the left by $2\pi / Nb$. As for the other inductances, L_{r1B} and L_{r1C} are identically reproduced, but shifted to the right by $2\pi/3$. The mechanical angle of skewing of the rotor bars is $\gamma = \pi/14$ rad, which is selected equal to one stator slot pitch, and the width of slot opening $\beta = \pi/36$.

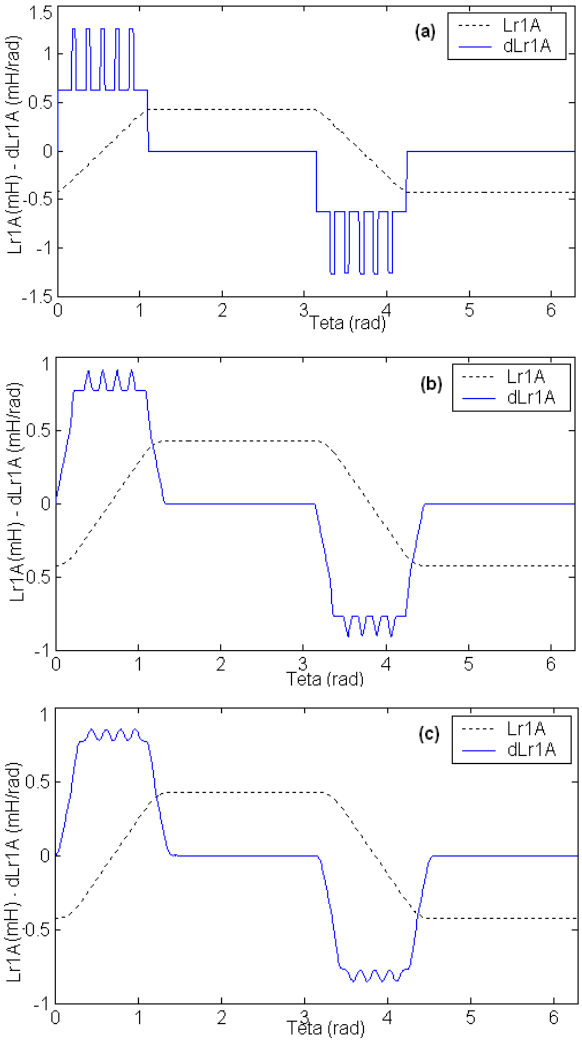

Fig. 1. Mutual inductance between stator phase A and rotor loop r_1.

a - without skew and slot opening.
b - with skew and without slot opening.
c- with skew and slot opening.

By solving the system of differential equations representing the induction machine, it is possible to simulate the dynamic operation of the machine.

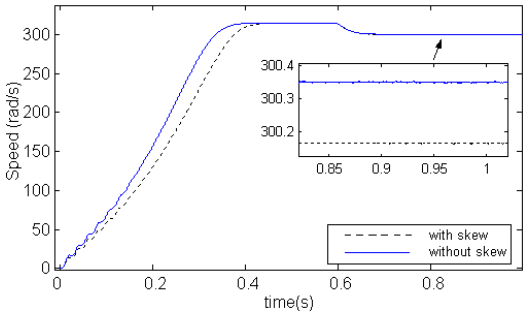

Fig. 2. Speed without rotor skew *and with* rotor skew.

Fig. 2 shows the transient dynamic start up behaviors of the induction motor under no load condition. At t=0.6s load is applied. The use of skewing reduces the average value and the oscillations of the speed at steady state [13].

Fig. 3 shows the transient dynamic start up behaviors of the induction motor under no load condition. At t=0.6s load is applied. It is clear that the use of skewing reduce the parasitic torque but it does not eliminate completely [8], [9], [10]. It is of course, to eliminate such effects that skew is employed in the real machines. The average torque has conserved the same value; it may be due to additional forces that the model can't take into account.

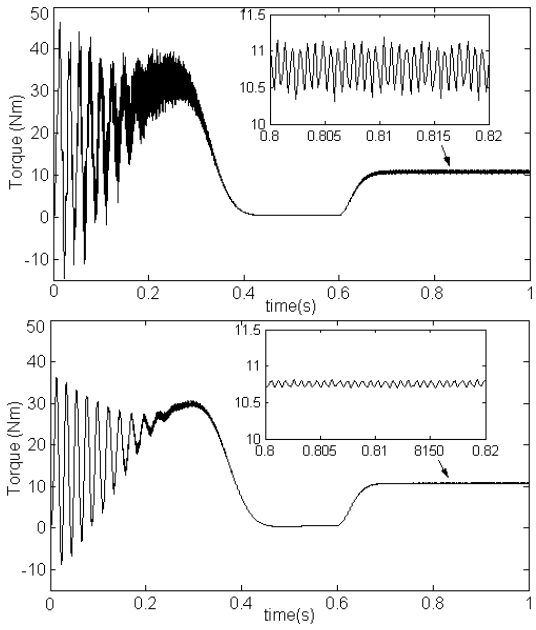

Fig. 3. Torque without rotor skew (top) and with rotor skew (bottom).

Fig. 4 shows the stator current at steady state for a loaded machine as a result of simulation analysis. Once again, if skew is neglected a slot ripples rise in the computed results.

The spectra of the stator current of a loaded machine are shown in Fig. 5. It is obvious that besides the supply frequency component, only two higher frequency components exist around the PSH1,2 as was predicted by:

$$f_{slot} = \left[\frac{N_b}{p}(1-s) \pm 1 \right] f_s \qquad (14)$$

where f_s represents the supply frequency, s the slip, N_b the number of rotor slots, and p is the pole-pair number. The magnitude of frequency associated to 1288.4Hz (1287.7Hz) and 1388.4Hz (1387.7Hz) are modified with the skewing. The use of skew reduces clearly the amplitude of slot harmonics [11].

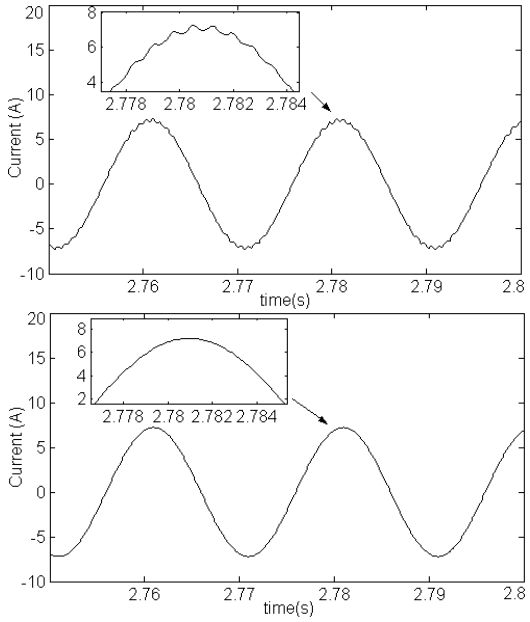

Fig. 4. Stator current without rotor skew (top) and with rotor skew (bottom) at steady state.

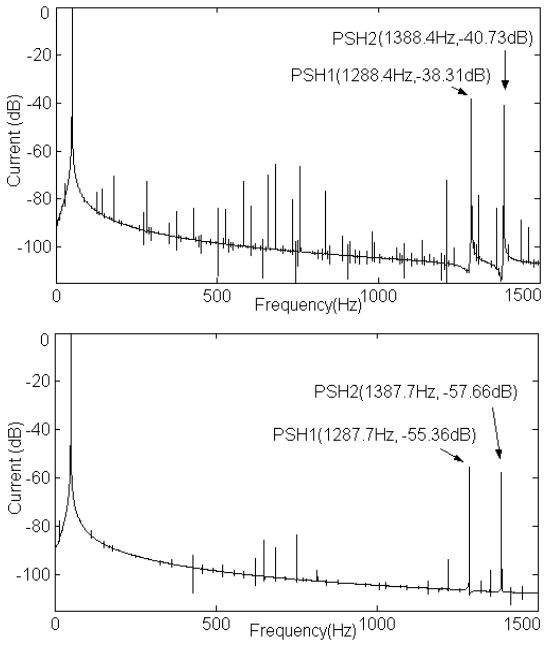

Fig. 5. Spectra content of stator current without rotor skew (top) and with rotor skew (bottom) for healthy machine.

In fig. 6, the spectra content of stator current with one broken bar are presented, for the skewed and unskewed rotor. In case of broken rotor bars, the rotor is electrically asymmetric and the backward rotating field is created. The current spectrum reveals sidebands expected around the supply frequency given by:

$$f_{bb1} = \left[(1 \pm 2s)\right] f_s \qquad (15)$$

In order to have a better understanding of rotor broken bar, it may be necessary to examine the higher frequency components of the frequency spectra. When we took into account the space harmonics, additional sidebands appear as was predicted by [12]:

$$f_{bb2} = \left[\frac{k}{p}(1-s) \pm s)\right] f_s \qquad (16)$$

where, k/p = 1,3,5,7, ….

It is noticed that the amplitude of the harmonics was reduced by the rotor skew, especially at high frequencies. Moreover, the slot harmonics were not affected clearly by the broken bars.

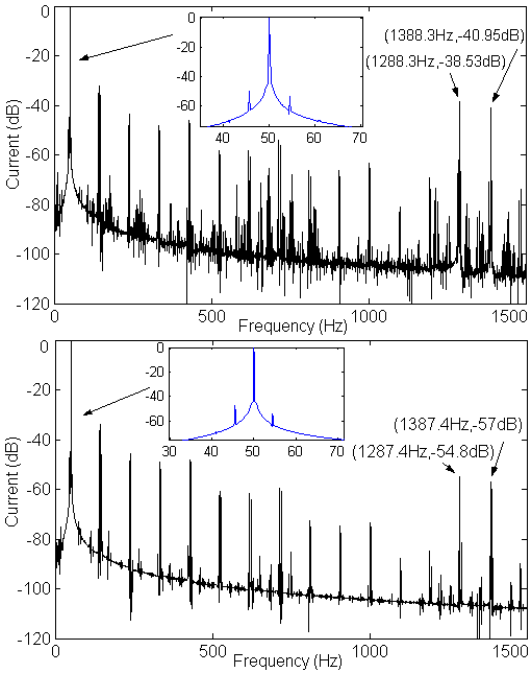

Fig. 6. Spectra content of stator current without rotor skew (top) and with rotor skew (bottom) for one broken rotor bars.

For including the harmonics of the power supply, we have injected the real signal resulting from the acquisition. In fig.7, the spectrum of stator current with one broken bar is presented, for the skewed rotor.

In fig. 7, we can notice the presence of the principal slots harmonics (PSH) and harmonics due to the power supply.

V- EXPERIMENTAL RESULTS

The experimental tests were carried out on an experimental bench within the laboratory of the GREEN-UHP in Nancy in France (Fig. 8). The test-motor used in the experimental investigation is the same used in simulation. Several rotors of identical type could be interchanged. Each of them is a single squirrel cage type with 28 rotor bars. Separately excited DC

generator feeding a variable resistor provides a mechanical load.

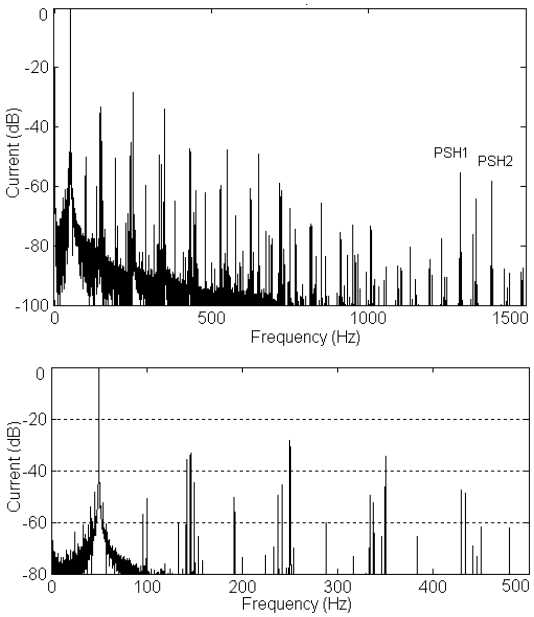

Fig. 7. Spectra content of stator current with one broken bar (top), frequency 0 to500Hz (bottom).

Initially, the voltages and the line currents measurements are taken for the motor operating at the nominal rate. For these two variables, the sampling frequency is 2 kHz, and each data length is equal to 2^{18} samples. Then the Fast Fourier Transform with a Henning's window is computed and the power spectrum of the current phase is plotted. The spectrum is drawn in the logarithmic magnitude scale and normalized format. The magnitude of the fundamental is assigned to the value of 0 dB.

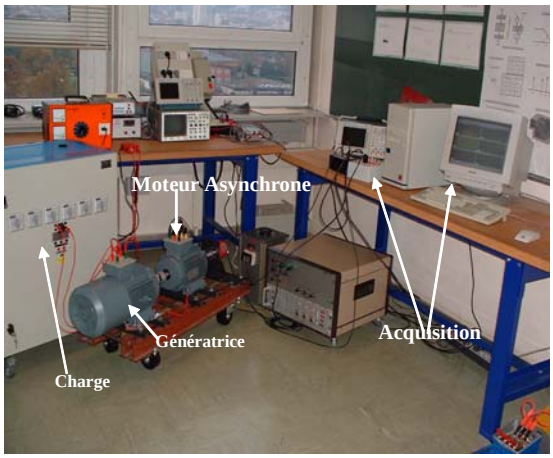

Fig. 8. experimental bench used.

The spectrum of fig. 9 shows that even for a motor in a healthy state, there are always frequency components but of low amplitudes , this is due to the natural asymmetry of the motor, and on the other hand from the power supply. We notice the presence of the slot harmonics in addition to the harmonics due to saturation.

As envisaged during simulation, we show the presence of the harmonics components of high frequencies. The spectra of fig. 10 shows that for a motor with one broken bar, the stator current frequency described by (15) and (16) can be detected over the observation bandwidth between 0 Hz and 500 Hz.

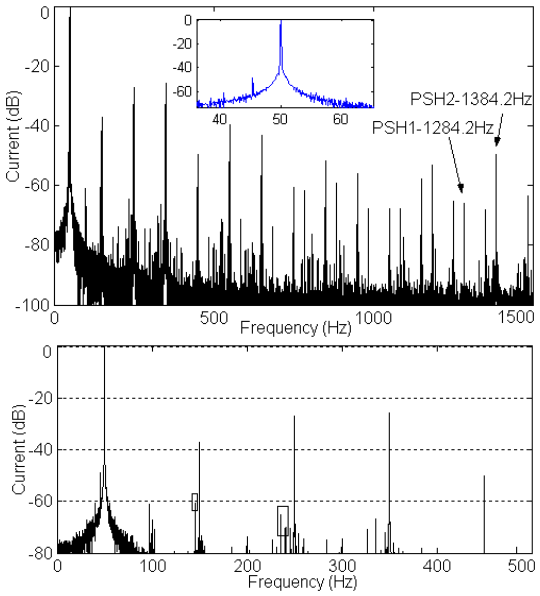

Fig. 9. Spectra content of stator current with healthy motor (top), frequency 0to500Hz (bottom).

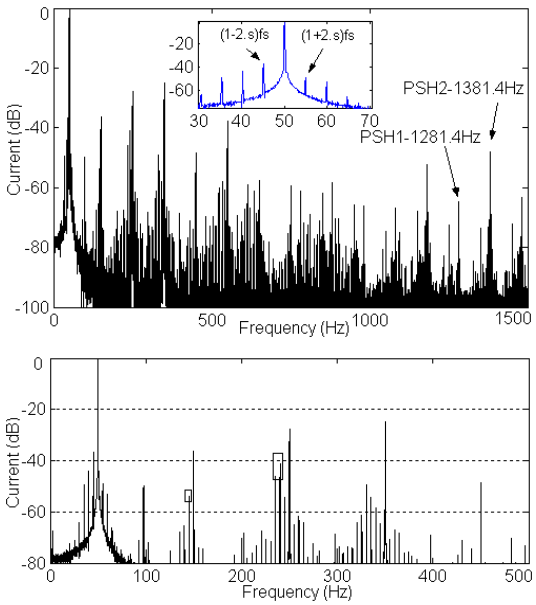

Fig. 10. Spectra content of stator current with one broken bar (top), frequency 0to500Hz (bottom).

The spectrum of fig. 9 shows that even for a motor in a healthy state, there are always frequency components but of low amplitudes , this is due to the natural asymmetry of the motor, and on the other hand from the power supply. We notice the presence of the slot harmonics in addition to the harmonics due to saturation. As envisaged during simulation, we show the presence of the harmonics components of high frequencies. The spectra of figure. 10 shows that for a motor with one broken bar, The stator current frequency described by (15) and (16) can be detected over the observation bandwidth between 0 Hz and 500 Hz.

By comparing the spectra resulting from the motor with one broken bar of the experimental test and simulation (Fig. 7 and Fig. 10), we can notice that the additional frequencies which appear in the spectrum resulting from the simulation of the motor supplied with the real signal resulting from acquisition, are due primarily to the harmonics of times contained in the supply voltage and in particular frequencies 150Hz and 250Hz, what enables us to say that the differences with simulation and the practice results are mainly in the approximations adopted at the level of the power supply.

V. CONCLUSION

This paper has presented an analytical approach applied to the induction motor with an extension of modified winding function approach taking into account the influence of rotor skew, and the broken rotor bars. Comprehensive experimental results verifying the developed theory are also presented. The effects of rotor skew were investigated. The torque ripples are reduced by the skewing, but not eliminate completely. The presence of skew in an induction motor produce an axial variation in the magnetic field witch is not taken into account by the model. Permeance variation due to saturation, rotor and stator slotting, loading have strong influence on the magnitude of the detected harmonics components.

APPENDIX

- Machine parameters: $g = 0.000172m$, *Nb=28* , *Ne=36,* $r = 0.0516m$, $w = 80$, $l = 0.125m$, L_b = *0.000172H,* L_e *=0.009594H,* $R_s = 2.86\Omega$, $R_b = 2.856\text{e-}5\Omega$, $R_e = 1.8560\text{e-}005\Omega$, $J = 0.023976\,kgm^2$, $\gamma = \pi/14 rad$. $\beta = \pi/36$.

REFERENCES

[1] A. H. Bonnett and G. C. Soukup, "Cause and Analysis of Stator and Rotor Failures in Three-Phase Squirrel-Cage Induction Motors", *IEEE Transactions on Industry Applications*, Vol. 28, No 4, pp. 921-937, July/August 1992.

[2] M.E.H. Benbouzid, "A review of induction motors signature analysis as a medium for faults detection" *IEEE Transactions on Industrial Electron*ics, Vol. 47, N°.5, pp. 984-993, October 2000.

[3] G.Bossio, C.D. Angelo, J.Solsona, G. García and MI. Valla, "A 2-D Model of the induction machine : Extension of the modified winding function approach," *IEEE Transactions on Energy Conversion*, vol. 19, no. 1, pp. 144-150, Mars 2004.

[4] A. Ghoggal, M. Sahraoui, A. Aboubou, S.E. Zouzou, "A 2-D model of induction machine dedicated to fault detection: extension of the modified winding function," PCSE.05-Université d'Oum-elbouaghi. 9-11,Mai 2005.

[5] J. Faiz, I. Tabatabaei, " Extension of Winding Function Theory for Non uniform Air Gap in Electric Machinery," IEEE *Transactions on Magnetics*, Vol. 38, N°.6, pp. 3654-3657, November 2002.

[6] M. G. Joksimovic, D. M. Durovic, J. Penman and N. Arthur," Dynamic simulation of dynamic eccentricity in induction machines-Winding function approach," *IEEE Transactions on Energy Conversion*, vol. 15, no. 2 , pp. 143-148, June 2000.

[7] H. A Toliyat, T.A Lipo," Transient Analyse of Induction Machines Under Stator, Rotor Bar and End Ring Faults," *EEE Transactions on Energy Conversion*,Vol.10, N°.2, pp.241-249, June1995.

[8] H. Kometani, S. Sakabe, and K. Nakanishi , " 3-D Electro-magnetic analysis of a cage induction motor with rotor skew," *IEEE Transactions on Energy Conversion*, vol. 11, no. 2, pp. 331-337, June 1996.

[9] H. C. Lai and D. Rodger, "Modelling rotor skew in induction machines using 2d and 3D finite element schemes," *IEEE International Electric Machines and Drives Conference record*, page WB3, 5.1-5.3, May 1997.

[10] S. Williamson, T. J. Flack and A. F. Volshenk , "Representation of skew in time-stepped tow dimensional finite–element models of electrical machines ," IEEE *Transactions on Industry Applications*, Vol. 31,pp.1009-1015, September / October 1995.

[11] A. Tenhunen and A. Arkkio , "Modelling of induction machines with skewed rotor slots," *Proceedings on Electric Power Appl*ications, Vol.148, no.1, pp.45-50, January 2001.

[12] W. Deleroi, "Broken Bar in Squirrel-Cage Rotor of an Induction Motor. Part I: Description by Superimposed Fault-Currents," *Archiv Fur Elektrotechnik*, Vol. 67, pp. 91–99, 1984.

[13] S.E. Zouzou, A. Ghoggal, A. Aboubou, M. Sahraoui and H. Razik, "Modelling of induction machines with skewed rotor slots dedicated to rotor faults," *In proceeding of IEEE Sdemped 2005*,Vienna, Austria, 7-9 Sept. 2005.

[14] A Ghoggal, M. Sahraoui, A. Aboubou, S.E. Zouzou, and H. Razik, "An improved model of induction machine dedicated to faults detection," *In proceeding of IEEE ICIT 2005*, Hang Kong, China, 15-17 Dec. 2005.

[15] A Ghoggal, S.E. Zouzou, A. Aboubou, M. Sahraoui, "A 2-D model of induction machine dedicated to faults detection," *JES, lournal of electric systems*, Oum-Elbouaghi University, Vol. 1, pp. Dec. 2005.